Tandem Dehydrogenation of Ammonia Borane and Hydrogenation of Nitro/Nitrile Compounds Catalyzed by Graphene–Supported NiPd Alloy Nanoparticles

7 AUTHORS, INCLUDING:

Onder Metin
Ataturk University
54 PUBLICATIONS **1,482** CITATIONS

SEE PROFILE

Adriana Mendoza-Garcia
Brown University
16 PUBLICATIONS **94** CITATIONS

SEE PROFILE

Mehmet Serdar Gültekin
Ataturk University
33 PUBLICATIONS **377** CITATIONS

SEE PROFILE

Tandem Dehydrogenation of Ammonia Borane and Hydrogenation of Nitro/Nitrile Compounds Catalyzed by Graphene-Supported NiPd Alloy Nanoparticles

Haydar Göksu,[†,§,∥] Sally Fae Ho,[‡,∥] Önder Metin,*[,†] Katip Korkmaz,[†] Adriana Mendoza Garcia,[‡] Mehmet Serdar Gültekin,[†] and Shouheng Sun*[,‡]

[†]Department of Chemistry, Faculty of Science, Atatürk University, 25240 Erzurum, Turkey
[‡]Department of Chemistry, Brown University, Providence, Rhode Island 02912, United States
[§]Kaynasli Vocational College, Düzce University, Düzce 81900, Turkey

Ⓢ *Supporting Information*

ABSTRACT: We report a facile synthesis of monodisperse NiPd alloy nanoparticles (NPs) and their assembly on graphene (G) to catalyze the tandem dehydrogenation of ammonia borane (AB) and hydrogenation of R-NO$_2$ and/or R-CN to R-NH$_2$ in aqueous methanol solutions at room temperature. The 3.4 nm NiPd alloy NPs were prepared by coreduction of nickel(II) acetate and palladium(II) acetylacetonate by borane-*tert*-butyl-amine in oleylamine and deposition on G via a solution phase self-assembly process. G-NiPd showed composition-dependent catalysis on the tandem reaction with G-Ni$_{30}$Pd$_{70}$ being the most active. A variety of R-NO$_2$ and/or R-CN derivatives were reduced selectively into R-NH$_2$ via G-Ni$_{30}$Pd$_{70}$ catalyzed tandem reaction in 5−30 min reaction time with the conversion yields reaching up to 100%. Our study demonstrates a new approach to G-NiPd-catalyzed dehydrogenation of AB and hydrogenation of R-NO$_2$ and R-CN. The G-NiPd NP catalyst is efficient and reusable, and the reaction can be performed in an environment-friendly process with short reaction times and high yields.

KEYWORDS: *alloy nanoparticles, tandem reaction, dehydrogenation, hydrogenation, nitro/nitrile compounds, primary amines*
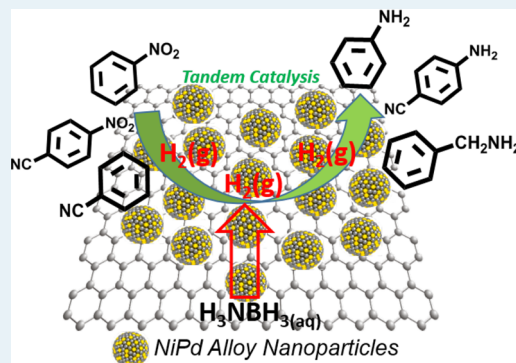
1. INTRODUCTION

Aromatic and aliphatic primary amines (denoted as R-NH$_2$) are an important class of compounds used as intermediates in the synthesis of numerous pharmaceutical, dye, polymer, and natural products.[1] R-NH$_2$ compounds are often synthesized by the reductive amination of aldehydes and alcohols in the presence of a hydrogen source. Alternatively, the amines can be prepared by direct hydrogenation of aromatic or aliphatic nitro (R-NO$_2$) and nitrile (R-CN) compounds in the presence of noble metal catalysts under high hydrogen pressures and high temperatures.[2−4] To create more environmentally benign conditions, alcohols such as ethanol,[5] isopropanol,[6] and glycerol[7] have been used as alternative hydrogen sources. However, the alcohol-initiated hydrogenation reactions are slow and have low reaction selectivity. Recently, ammonia borane (AB, NH$_3$·BH$_3$) has become a popular choice as a hydrogen source for the reduction process due to its high volume/mass hydrogen density, nontoxicity, and high-solubility in water.[8] It has been used to reduce C=C, C=N, and C=O bonds in aqueous solutions under ambient conditions.[9]

Palladium based catalysts have been shown to facilitate the dehydrogenation of AB[10] and selectively hydrogenate a variety of substrates.[11] Therefore, a catalytic tandem reaction in which Pd serves a dual role to catalyze the dehydrogenation of AB and hydrogenate R-NO$_2$ or R-CN would be an efficient way to generate R-NH$_2$. Considering the enhanced catalytic performance and selectivity of bimetallic NPs demonstrated in hydrogenation reactions[12] and the dehydrogenation of AB,[13] as well as the role a nickel catalyst plays to selectively hydrogenate nitro or nitrile groups to R-NH$_2$,[14] we started to explore bimetallic MPd NPs, especially NiPd NPs, as the efficient tandem reaction catalysts. In this article, we report a facile synthesis of NiPd NPs and their assembly on graphene (G) to catalyze the tandem AB dehydrogenation and hydrogenation of R-NO$_2$ and/or R-CN to R-NH$_2$ in aqueous methanol solutions at room temperature. Recently, we reported the synthesis of MPd (M: Co or Cu) NPs by reduction of PdBr$_2$ and M(acac)$_2$ (acac = acetylacetonate) at 260 °C in oleylamine (OAm) and trioctylphosphine (TOP).[15] The TOP-coated CoPd NPs were active catalysts for the hydrolysis of AB.[16] However, they were inactive for the hydrogenation reaction, and the activation process to remove TOP led to the
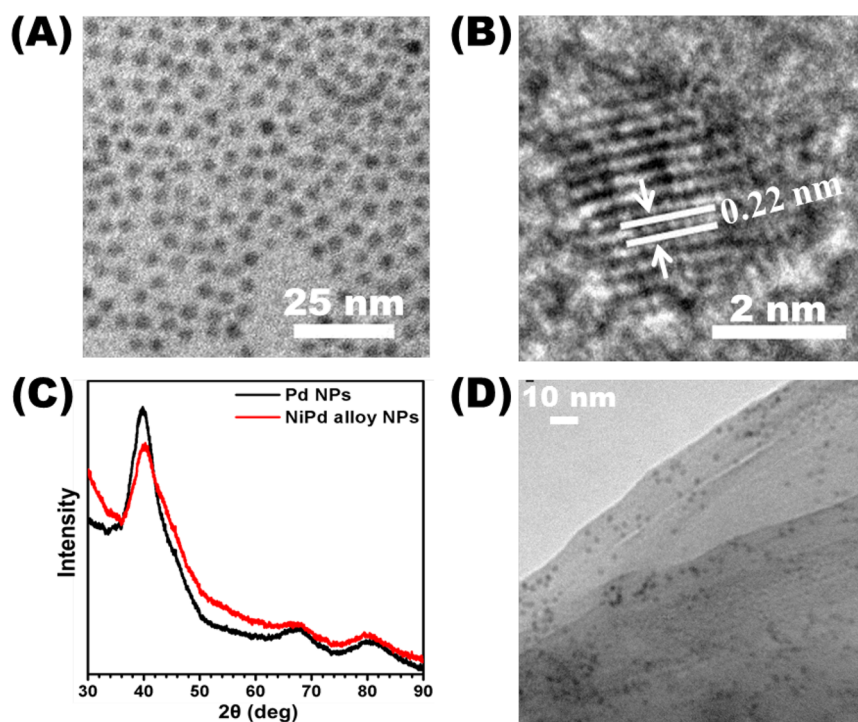
Figure 1. (A) TEM and (B) HRTEM images of $Ni_{30}Pd_{70}$ NPs, (C) XRD patterns of Pd and NiPd NPs, and (D) the representative TEM image of NiPd NPs deposited on graphene.

degradation of NP quality. To improve MPd catalysis, we developed a new non-TOP route to MPd NPs. In this synthesis, NiPd NPs were prepared by coreduction of Ni and Pd-salt precursors by borane-*tert*-butylamine (BBA) in OAm. These NiPd NPs were active not only for AB dehydrogenation but also for the hydrogenation of $R-NO_2$ and/or R-CN to RNH_2. Especially, when the NiPd NPs were deposited on G, they became a highly efficient catalyst for tandem AB dehydrogenation and hydrogenation reactions in aqueous solution at room temperature. We tested the tandem reaction on a variety of $R-NO_2$ and/or R-CN and found that NO_2 and CN bonds were reduced selectively to produce $R-NH_2$ in 5−30 min of reaction time with the conversion yields reaching up to 100%.

2. RESULTS AND DISCUSSION

Monodisperse NiPd alloy NPs were synthesized via the coreduction of nickel(II) acetate, $Ni(ac)_2$, and palladium(II) acetylacetonate, $Pd(acac)_2$, by BBA in OAm and 1-octadecene (ODE). In the synthesis, OAm acted as the surfactant, BBA served as the reducing agent, and ODE was used as a solvent. The metal contents of the NiPd alloy NPs were analyzed by inductively coupled plasma-atomic emission spectroscopy (ICP-AES). In the current reaction conditions, $Ni_{30}Pd_{70}$ NPs were obtained by reducing 0.2 mmol of $Ni(ac)_2 \cdot H_2O$ and 0.2 mmol of $Pd(acac)_2$. $Ni_{20}Pd_{80}$ NPs were synthesized by changing the Ni:Pd molar ratio to 0.1:0.25. Figure 1A shows a representative TEM image of the as-synthesized of $Ni_{30}Pd_{70}$ NPs. The NPs are monodisperse with a mean particle size of 3.4 ± 0.3 nm in diameter. Figure 1B is a representative HRTEM image of a single NiPd NP in which the polycrystalline nature of the NP is seen. The lattice fringe distance is at 0.22 nm, which is closer to the lattice spacing of the (111) planes of the face centered cubic (fcc) Pd (0.223 nm) and larger than that of the fcc-Ni (0.203 nm), indicating that the

Pd-rich NiPd structure is indeed formed. Figure 1C shows the XRD patterns of Pd and NiPd NPs. By using the Scherrer equation, we calculated the crystal size of the NiPd NPs to be 2.8 nm. This size is smaller than that measured from TEM, indicating that the as-synthesized NPs are in polycrystalline structure. Furthermore, the (111) peak shifts to a higher diffraction angle $(2\theta = 40.3°)$ compared to that of the corresponding peak from the Pd NPs $(2\theta = 39.5°)$, indicating that the (111) lattice spacing of the NiPd NPs is smaller than that of the Pd NPs. This is consistent with what is seen from the HRTEM analysis of the NiPd NP (Figure 1B), confirming that NiPd NPs have a solid solution structure.

The NiPd NP size and composition could also be controlled by the temperature at which the metal precursors were injected into the reaction. For example, the injection of 0.30 mmol of $Ni(ac)_2$ and 0.25 mmol of $Pd(acac)_2$ into the BBA solution at 75 °C yielded $3.3 + 0.3$ nm $Ni_{35}Pd_{75}$ NPs (Figure S1-A, Supporting Information), whereas the injection at 125 °C gave 3.9 ± 0.4 nm $Ni_{50}Pd_{50}$ NPs (Figure S1−B, Supporting Information). It is noteworthy to mention that alloying Ni with Pd is thermodynamically difficult and that the synthesis of alloy NPs with the higher Ni:Pd ratio could not be achieved at temperatures higher than 125 °C. The large lattice mismatch between Ni and Pd $(9.4−10\%)[17]$ might make it difficult for the two metals to intermix well together, which is different from the formation of CoPd and CuPd, where Co/Pd $(4.5\%)[12c]$ and Cu/Pd $(7.1\%)[18]$ have smaller lattice mismatches. Previous studies also indicate that Ni and Pd have difficulty forming a solid solution and that NiPd alloy NPs are often produced by the Ni/Pd interdiffusion of the preformed Pd/Ni core/shell NPs at temperatures greater than 265 °C.[19,20]

To perform the catalytic test, we deposited the NiPd NPs on graphene (G) through the sonication of an ethanol dispersion of G and a hexane dispersion of NiPd NPs, similar to what is reported in the assembly of FePt NPs on G,[21] producing G-

NiPd. Figure 1D shows the TEM image of the as-prepared G-NiPd catalyst. The NiPd NPs are well-dispersed on the G surface, and their initial morphology and size remain preserved during the assembly process. Without any further surfactant removal treatment, this G-NiPd catalyst was tested directly for the tandem reaction. We first used nitrobenzene (or its simple derivative) as a model compound to demonstrate G-NiPd NP catalysis for the tandem dehydrogenation of AB and hydrogenation of R-NO$_2$ and to obtain the optimum reaction conditions. We tested the catalytic tandem reactions at room temperature in different solvents including water, methanol, ethanol, and their mixtures at various ratios and found the mixed solvent of methanol/water (v/v = 7/3) to be the best solvent combination to convert nitrobenzene (1) to aniline (2). Among the three different G-NiPd catalysts tested for the tandem reduction, G-Ni$_{30}$Pd$_{70}$ showed the highest efficiency with high amine conversion yields in short reaction times. Therefore, the G-Ni$_{30}$Pd$_{70}$ catalyst was used to catalyze the tandem AB dehydrogenation and hydrogenation reactions.

We further studied the AB effect (different AB/nitrobenzene ratios) on the catalytic tandem reactions (Table S1, Supporting Information). The conversion yields were increased with increasing AB/nitrobenzene ratios, reaching the maximum when the ratio was at 3. We also studied the support effect on Ni$_{30}$Pd$_{70}$ catalysis. These NPs supported on either a conventional carbon support (C-Ni$_{30}$Pd$_{70}$) (Figure S2, Supporting Information) or aluminum oxide nanopowder (Al$_2$O$_3$–Ni$_{30}$Pd$_{70}$) (Figure S3, Supporting Information) were active catalysts for the tandem reaction to reduce p-nitrophenol to 4-aminophenol, but the conversion yields were low (54% and 55%, respectively). G has an atomically flat surface and high adsorption power for organic molecules, and when G was used as a support, both the NiPd NPs and reactants would be more strongly adsorbed on G than on C or Al$_2$O$_3$, and the G-Ni$_{30}$Pd$_{70}$ NPs exhibit much increased catalytic efficiency due to the high local reactant concentration. Finally, we should mention that the NP catalyst is needed for the tandem reaction as no product was obtained over 24 h when the reaction was performed in the absence of the catalyst. From these tests, we can conclude that 3 equiv of AB in methanol/water mixture (v/v = 7/3) at room temperature is the optimum reaction condition for the G-Ni$_{30}$Pd$_{70}$ NPs to catalyze the tandem reaction.

Table 1 summarizes the results obtained from G-Ni$_{30}$Pd$_{70}$ catalyzed tandem reactions of various R-NO$_2$ compounds. All aromatic or aliphatic nitro compounds tested were converted into the respective primary amines with excellent conversion yields in 5−30 min at room temperature.[22] For example, nitrobenzene (1) was reduced to aniline (2) quantitatively in 5 min (Table 1, entry 1). The NO$_2$ groups in p-methyl, o-methoxy, m-hydroxyl, and p-hydroxyl-nitrobenzenes (3, 5, 7, and 9) were also reduced into the related amine products (4, 6, 8, and 10) in nearly quantitative conversion yields in 5 min (Table 1, entries 2−5). The catalytic reaction could be easily extended to 2-nitro-naphthyl (11), 3-nitro-9H-fluorene (13), and 2-chloro-5-nitropyridine (15) compounds, which were all converted to the respective amine derivatives (12, 14, and 16) with the conversion yields higher than 95% in 5 min (Table 1, entries 6−8). These amine derivatives with heteroaromatic structures are especially important medicinal agents due to their potent antimicrobial and insecticidal properties.[23]

For 1,3-dinitrobenzene (17), both NO$_2$ groups were reduced quantitatively to NH$_2$ (18) in 5 min (Table 1, entry 9).

Table 1. G-Ni$_{30}$Pd$_{70}$-Catalyzed Tandem Reaction of Various R-NO$_2$ Compounds[a]

Entry	Substrate	Product	Yield %	Time (min)
1	(1)	(2)	>99	5
2	(3)	(4)	>99	5
3	(5)	(6)	>99	5
4	(7)	(8)	>99	5
5	(9)	(10)	>99	5
6	(11)	(12)	95	5
7	(13)	(14)	>99	5
8	(15)	(16)	>99	5
9	(17)	(18)	>99	5
10	(19)	(18)	>99	30
11	(20)	(21)	>99	10
12	(22)	(23)	>99	15
13	(24)	(25)	>99	5
14	(26)	(27)	>99	5
15	CH$_3$-NO$_2$ (28)	CH$_3$-NH$_2$ (29)	>99	5
16	C$_2$H$_5$-NO$_2$ (30)	C$_2$H$_5$-NH$_2$ (31)	>99	5

[a]Reaction conditions: 1 mmol substrate, 3 mmol NH$_3$BH$_3$, 4 mg G-Ni$_{30}$Pd$_{70}$ catalyst (25 wt % metal content), 10 mL of water/methanol (v/v = 3/7), and room temperature.

Reduction of *meta*-amino-nitrobenzene (19) was a little slower process, reaching 100% conversion after 30 min of reaction (Table 1, entry 10). Other amino-nitrobenzenes (20 and 22) were reduced similarly to 1,3-dinitrobenzene, producing the corresponding diamine products (Table 1, entries 11 and 12). The selective reduction of -NO$_2$ was better demonstrated in aromatic compounds bearing other reducible substituents such as 1-bromo-4-nitrobenzene (24) and methyl 2-hydroxy-4-

nitrobenzoate (**26**). They were all reduced to the related amine products (>99% conversion in 5 min) (Table 1, entries **13** and **14**), and the Br- or ester group showed no obvious effect on the NO_2 reduction kinetics. The tandem reaction could be further extended to the simple aliphatic nitro compounds such as methyl nitro (**28**) and ethyl nitro (**30**) compounds that were all converted to the related primary amines quantitatively (**29** and **31**) in 5 min (Table 1, entries **15** and **16**). Our synthetic results demonstrate that the G-NiPd NP-catalyzed tandem reaction is highly efficient and selective for $-NO_2$ reduction into $-NH_2$ and that other functional groups around NO_2 have little effect on the reduction outcome. This is also consistent with the literature observations that $-NO_2$ is much easily reduced.[24]

The G-NiPd NPs were equally active in catalyzing the tandem reaction to reduce aromatic and aliphatic nitrile compounds to the corresponding amines in conversion yields up to 100% within 10 min (Table 2, entries 1−3). However,

Table 2. G-Ni$_{30}$Pd$_{70}$-Catalyzed Tandem Reduction of Nitrile and/or Nitro Compounds[a]

$$R\text{-}CN \xrightarrow[\text{water/methanol (v/v:3/7), RT}]{\substack{\text{4 mg G-Ni}_{30}\text{Pd}_{70} \\ \text{3 mmol NH}_3\text{BH}_3}} R\text{-}CH_2NH_2$$

Entry	Substrate	Product	Yield %	Time (min.)
1	⬡—CN (**32**)	⬡—CH$_2$NH$_2$ (**33**)	>99	10
2	CH$_3$CH$_2$CN (**34**)	C$_2$H$_5$NH$_2$ (**35**)	98	5
3	(CH$_3$)$_2$CH-CN (**36**)	(CH$_3$)$_2$CH-CH$_2$NH$_2$ (**37**)	97	5
4	o-CN,NO$_2$-benzene (**38**)	o-CN,NH$_2$-benzene (**39**)	98	10
5	O$_2$N—⬡—CN (**40**)	H$_2$N—⬡—CN (**41**)	94	10
6	O$_2$N—⬡(CN)$_2$ (**42**)	H$_2$N—⬡(CN)$_2$ (**43**)	97	5
7	NC—⬡—NHC(O)CH$_3$ (**44**)	H$_2$NCH$_2$—⬡—NHC(O)CH$_3$ (**45**)	40 / 90	2 h / 12 h

[a]Reaction conditions: 1 mmol substrate, 3 mmol NH_3BH_3, 4 mg G-Ni$_{30}$Pd$_{70}$ catalyst (25 wt % metal content), 10 mL of water/methanol (v/v = 3/7), and room temperature.

when the starting compounds bearing both -CN and -NO_2 moieties, such as cyano-nitrobenzene, only NO_2, not CN, was reduced to NH_2 (Table 2, entry 4−6). To elucidate this selectivity, we performed additional tests on *p*-aminobenzonitrile (**41**) and its acetated derivative *p*-cyanophenylacetamide (**44**). We found that when (**41**) was used as a substrate, only 3% conversion was achieved in 2 h, and longer reaction times (up to 12 h) did not lead to any notable increase on the yield of the corresponding amine derivative *p*-aminomethylaniline. When *p*-cyanophenylacetamide (**44**) was present in the tandem reaction condition, the -CN was more easily reduced to -NH_2 with the conversion yield up to 90% after 12 h of reaction. As a comparison, the tandem reaction of AB with the mixture of nitrobenzene (**1**) and benzonitrile (**32**) (1:1 molar ratio) yielded the respective amines (**2** and **33**) quantitatively. From these experimental results, we conclude that while the G-NiPd-

catalyzed tandem reaction is very active and selective to reduce -NO_2 to -NH_2, the same reaction condition has very limited power to reduce -CN when this -CN is conjugated with -NO_2 and/or -NH_2 in the arene structure. This limited reduction is likely caused by the electronic/conjugation effect of -NH_2 on -CN, which stabilizes the -CN against further reduction.

The G-NiPd NPs and their catalysis on the tandem reaction can be compared favorably with other methods reported for the reduction of R-NO_2, as shown in Table S2 (Supporting Information). In general, the G-NiPd-catalyzed reactions proceed much faster at room temperature. Other methods require longer time and/or higher reaction temperatures. For example, Au NPs supported on magnesium oxide (MgO-Au) catalyzed $NaBH_4$ reduction of nitrobenzene, producing aniline in 85% yield after 1 h of reaction at room temperature,[25] and in the presence of Au/TiO$_2$, AB reduced nitrobenzene to aniline in 92% yield after 30 min at 25 °C.[26] As a comparison, the G-NiPd NP catalyzed reaction converted nitrobenzene to aniline in >99% yield after only 5 min of reaction at room temperature.

An extra benefit of using the new G-NiPd catalyst for tandem AB dehydrogenation and R-NO_2/R-CN hydrogenation is that it is stable and reusable. We tested its durability by performing the tandem reaction on *p*-nitrophenol. The catalyst was separated after each reaction and washed with water/methanol for the next round of reaction. After the fifth consecutive use, the catalyst still showed the conversion yield higher than 95% in the same reaction times. We believe that the high activity and stability of the G-NiPd catalyst stems from its stable dispersion in water/methanol and from the presence of a graphitic plane near the G-NiPd, which enriches all reactants around each NiPd NP, facilitating the tandem reaction.

3. CONCLUSIONS

In summary, we have reported a facile route to monodisperse 3.4 nm NiPd alloy NPs. Using solution-phase self-assembly, we deposited these NiPd NPs on the graphene (G) surface and demonstrated that the G-NiPd was efficient in catalyzing the tandem reaction of the dehydrogenation of AB and hydrogenation of R-NO_2 or R-CN to produce primary amines R-NH_2. The catalytic reactions were run in the aqueous methanol solutions at room temperature. In the series of aromatic or aliphatic nitro and/or nitrile compounds tested, they were all reduced to the respective primary amines with the excellent conversion yields in short reaction times (5−30 min). Compared to the known hydrogenation methods, our current approach has the following distinct advantages: (1) the catalyst is efficient, reusable, and cost-effective; (2) the tandem reaction can be performed in an environmentally friendly and safe manner (no stored/pressurized hydrogen is needed); (3) the reaction is easy to operate at ambient conditions with short reaction times and high yields; (4) the reduction is especially selective for R-NO_2; and (5) the reduction is also active for R-CN when there is no π-conjugated -NO_2 and -NH_2 copresent with -CN. It opens up a new avenue to selective reduction of R-NO_2 and/or R-CN to R-NH_2.

4. EXPERIMENTAL SECTION

Materials. The NP synthesis was carried out using standard airless procedures and commercially available reagents. All reagents were used as received. Oleylamine (OAm) (>70%), borane-*tert*-butylamine (BBA, 97%), palladium acetylacetonate (Pd(acac)$_2$, 99%), activated carbon (DARCO-100 mesh

particle size), aluminum oxide nanopowder (<50 nm (BET)), and all nitro and/or nitrile compounds used in the tandem reaction were purchased from Sigma-Aldrich and used as received. Nickel(II) acetate tetrahydrate (98%) was obtained from Strem Chemicals.

Characterization Methods. Samples for transmission electron microscopy (TEM) analysis were prepared by depositing a single drop of the diluted NP dispersion in hexane amorphous carbon-coated copper grids. Images were obtained on a Philips CM20 at 200 kV. High resolution TEM (HRTEM) images were obtained on a JEOL 2100F with an accelerating voltage of 200 kV. X-ray diffraction (XRD) patterns were collected on a Bruker AXS D8-advanced diffractometer with Cu Kα radiation (λ = 1.5418 Å). Inductively coupled plasma (ICP) elemental analysis measurements were carried out on a JY2000 Ultrace ICP atomic emission spectrometer equipped with a JY AS 421 autosampler and 2400g/mm holographic grating. For ICP analysis, an aliquot of the NPs in hexane was dried and subsequently dissolved in warm (~75 °C) aqua regia for 30 min to ensure complete dissolution of metal into the acid. The solution was then diluted with 2% HNO_3 solution for analysis. ^1H NMR and ^{13}C NMR spectra were recorded on a Bruker Avance DPX 400 MHz spectrometer.

Synthesis of NiPd Alloy NPs. In a typical synthesis of $Ni_{30}Pd_{70}$ NPs, 0.2 mmol of palladium(II) acetylacetonate ($Pd(acac)_2$) and 0.2 mmol of nickel(II) acetate tetrahydrate ($Ni(ac)_2 \cdot 4H_2O$) were dissolved in 3 mL of OAm. The precursor mixture was quickly injected into a mixture of 200 mg of BBA, 3 mL of OAm, and 7 mL of 1-octadecene (ODE) at 100 °C under magnetic stirring in an argon environment. The reaction was allowed to proceed for 1 h and cooled to room temperature. Then acetone/ethanol (v/v = 7/3) was added, and the NP product was separated by centrifugation at 9000 rpm for 10 min. The NPs were redispersed in hexane and then stored for further use.

Assembly of NiPd Alloy NPs on G. In a typical procedure, 10 mg of the NiPd NPs was dissolved in 5.0 mL of hexane and mixed with 30.0 mg of G in ethanol (60 mL). The ethanol/hexane mixture was sonicated for 2 h to ensure complete adsorption of NPs onto G. Then, the resultant mixture was centrifuged at 8000 rpm for 10 min, and the separated catalyst was washed with ethanol twice and dried under vacuum, giving G-NiPd. The NiPd NPs were also supported on activated carbon (C-NiPd) and aluminum oxide powder (Al_2O_3-NiPd) by using the same method and catalyst loading described above.

General Procedure for the Catalytic Tandem Reactions. The R-NO$_2$ or R-CN (1 mmol), G-NiPd catalyst (4 mg), and water/methanol (3:7) were stirred for 5 min in a 100 mL thermolysis tube at room temperature. Next, AB (3 mmol) was added to the reaction mixture, and the vessel was closed. The reaction was then continued under vigorous stirring at room temperature. The progress of the catalytic reaction was monitored by thin layered chromatography (TLC). Most reactions completed over the time period of 5−30 min. After completion of the reaction, the catalysts were removed by centrifugation at 7000 rpm and washed three times with water or methanol. Then, the catalysts were allowed to dry for further use. The solvent was removed by using a rotary evaporator. Finally, the crude residue was directly purified by column chromatography on silica gel using acetone. The yields of the reduced compounds were determined by ^1H and ^{13}C NMR

with D_2O, DMSO, CD_3OD, or $CDCl_3$ as the solvent depending on the product separated.

■ ASSOCIATED CONTENT

⑤ Supporting Information
TEM images of C-NiPd and Al_2O_3-NiPd catalysts, NMR spectra of amine compounds, and previous hydrogenation reactions. This material is available free of charge via the Internet at http://pubs.acs.org.

■ AUTHOR INFORMATION

Corresponding Authors
*E-mail: ometin@atauni.edu.tr.
*E-mail: ssun@brown.edu.

Author Contributions
$^\parallel$H.G. and S.F.H. contributed equally to this work.

Notes
The authors declare no competing financial interest.

■ ACKNOWLEDGMENTS

■ REFERENCES

(1) (a) Downing, R. S.; Kunkeler, P. J.; van Bekkum, H. *Catal. Today* **1997**, *37*, 121−136. (b) Ono, N. *The Nitro Group in Organic Synthesis*; Wiley-VCH: New York, 2001. (c) Kim, D.; Guengerich, F. P. *Annu. Rev. Pharmacol. Toxicol.* **2005**, *45*, 27−49. (d) Wang, K.; Guengerich, F. P. *Chem. Res. Toxicol.* **2013**, *26*, 993−1004.

(2) For a recent overview on the synthetic aspects of the catalytic reduction of nitroarenes, see Blaser, H. U.; Siegrist, U.; Steiner, H.; Studer, M. In *Fine Chemicals through Heterogeneous Catalysis*; Wiley-VCH: Weinheim, Germany, 2001; p 389.

(3) Blaser, H.-U.; Steiner, H.; Studer, M. *ChemCatChem* **2009**, *1*, 210−221.

(4) For reviews on transfer hydrogenation, see (a) Gladiali, S.; Mestroni, G. In *Transition Metals for Organic Synthesis*; Wiley-VCH: Weinheim, Germany, 2004; p 145. (b) Gladiali, S.; Alberico, E. *Chem. Soc. Rev.* **2006**, *35*, 226−236. (c) Samec, J. S. M.; Backvall, J.-E.; Andersson, P. G.; Brandt, P. *Chem. Soc. Rev.* **2006**, *35*, 237−248.

(5) Chandrappa, S.; Vinaya, K.; Ramakrishnappa, T.; Rangappa, K. S. *Synlett* **2010**, *20*, 3019−3022.

(6) Mohapatra, S. K.; Sonavane, S. U.; Jayaram, R. V.; Selvam, P. *Tetrahedron Lett.* **2002**, *43*, 8527−8529.

(7) (a) Wolfson, A.; Dlugy, C.; Shotland, Y.; Tavor, D. *Tetrahedron Lett.* **2009**, *50*, 5951−5953. (b) Gawande, M. B.; Rathi, A. K.; Branco, P. S.; Nogueira, I. D.; Velhinho, A.; Shrikhande, J. J.; Indulkar, U. U.; Jayaram, R. V.; Ghumman, C. A. A.; Bundaleski, N.; Teodoro, O. M. N. D. *Chem.—Eur. J.* **2012**, *18*, 12628−12632.

(8) (a) Peng, B.; Chen, J. *Energy Environ. Sci.* **2008**, *1*, 479−483. (b) Demirci, U. B.; Miele, P. *Energy Environ. Sci.* **2009**, *2*, 627−637. (c) Smythe, N. C.; Gordon, J. C. *Eur. J. Inorg. Chem.* **2010**, 509−521. (d) Umegaki, T.; Yan, J.-M.; Zhang, X.-B.; Shioyama, H.; Kuriyama, N.; Xu, Q. *Int. J. Hydrogen Energy* **2009**, *34*, 2303−2311.

(9) (a) Yang, X.; Fox, T.; Berke, H. *Chem. Commun.* **2011**, *47*, 2053−2055. (b) Yang, X.; Zhao, L.; Fox, T.; Wang, Z.-X.; Berke, H. *Angew. Chem., Int. Ed.* **2010**, *49*, 2058−2062. (c) Yang, X.; Fox, T.; Berke, H. *Tetrahedron* **2011**, *67*, 7121−7127.

(10) (a) Kılıç, B.; Sencanlı, S.; Metin, Ö. *J. Mol. Catal. A: Chem.* **2012**, *361−362*, 104−110. (b) Akbayrak, S.; Kaya, M.; Volkan, M.; Ozkar, S. *Appl. Catal., B* **2014**, *147*, 387−393. (c) Erdogan, H.; Metin,

O.; Ozkar, S. *Phys. Chem. Chem. Phys.* **2009**, *11*, 10519−10525. (d) Metin, Ö.; Sahin, S.; Özkar, S. *Int. J. Hydrogen Energy* **2009**, *34*, 6304−6313.

(11) (a) Niu, Y. H.; Yeung, L. K.; Crooks, R. M. *J. Am. Chem. Soc.* **2001**, *123*, 6840−6846. (b) Maegawa, T.; Takahashi, T.; Yoshimura, M.; Suzuka, H.; Monguchi, Y.; Sajiki, H. *Adv. Synth. Catal.* **2009**, *351*, 2091−2095. (c) Ueno, T.; Suzuki, M.; Goto, T.; Matsumoto, T.; Nagayama, K.; Watanabe, Y. *Angew. Chem., Int. Ed.* **2004**, *43*, 2527−2530.

(12) (a) Sankar, M.; Dimitratos, N.; Miedziak, P. J.; Wells, P. P.; Kielye, C. J.; Hutchings, G. J. *Chem. Soc. Rev.* **2012**, *41*, 8099−8139. (b) Liu, X.; Wang, D.; Li, Y. *Nano Today* **2012**, *7*, 448−466. (c) Singh, A. K.; Xu, Q. *ChemCatChem* **2013**, *5*, 652−676.

(13) (a) Singh, A. K.; Xu, Q. *ChemCatChem* **2013**, *5*, 3000−3004. (b) Jiang, H. L.; Umegaki, T.; Akita, T.; Zhang, X. B.; Haruta, M.; Xu, Q. *Chem.—Eur. J.* **2010**, *46*, 3132−3137. (c) Rachiero, G. P.; Demirci, U. B.; Miele, P. *Int. J. Hydrogen Energy* **2011**, *36*, 7051−7065. (d) Sun, D.; Mazumder, V.; Metin, Ö.; Sun, S. *ACS Catal.* **2012**, *2*, 1290−1295.

(14) (a) Shimizu, K.; Kon, K.; Onodera, W.; Yamazaki, H.; Kondo, J. N. *ACS Catal.* **2013**, *3*, 112−117. (b) Gowda, S.; Gowda, D. C. *Tetrahedron* **2002**, *58*, 2211−2213.

(15) Mazumder, V.; Chi, M.; Mankin, M.; Liu, Y.; Metin, Ö.; Sun, D.; More, K. L.; Sun, S. *Nano Lett.* **2012**, *12*, 1102−1106.

(16) Sun, D.; Mazumder, V.; Metin, Ö.; Sun, S. *ACS Nano* **2011**, *5*, 6458−6464.

(17) (a) Chang, C. *J. Magn. Magn. Mater.* **1991**, *96*, L1−L7. (b) Porte, L.; Phaner-Goutorbe, M.; Guigner, J. M.; Bertolini, J. C. *Surf. Sci.* **1999**, *424*, 262−270.

(18) Jin, M.; Zhang, H.; Zhong, X.; Lu, N.; Li, Z.; Xia, Z.; Kim, M. J.; Xia, Y. *ACS Nano* **2012**, *6*, 2566−2573.

(19) (a) Zhang, M.; Yan, Z.; Sun, Q.; Xie, J.; Jing, J. *New J. Chem.* **2012**, *36*, 2533−2540. (b) Son, S. U.; Jang, Y.; Park, J.; Na, H. B.; Park, H. M.; Yun, H. J.; Lee, J.; Hyeon, T. *J. Am. Chem. Soc.* **2004**, *126*, 5026−5027. (c) Metin, Ö.; Ho, S. F.; Alp, C.; Can, H.; Mankin, M. N.; Gültekin, M. S.; Chi, M.; Sun, S. *Nano Res.* **2013**, *6*, 10−18.

(20) Lee, K.; Kang, S. W.; Lee, S.; Park, K.-H.; Lee, Y. W.; Han, S. W. *ACS Appl. Mater. Interfaces* **2012**, *4*, 4208−4214.

(21) Guo, S.; Sun, S. *J. Am. Chem. Soc.* **2012**, *134*, 2492−2495.

(22) See Table S1 (Supporting Information) for the activities of various catalyst systems tested in the reduction of aromatic or aliphatic nitro compounds including the transfer hydrogenation route so far.

(23) (a) Patrick, G. L.; Kinsman, O. S. *Eur. J. Med. Chem.* **1996**, *31*, 615−624. (b) Nagashree, S.; Mallesha, L.; Mallu, P. *Pharma Chem.* **2013**, *5*, 50−55.

(24) (a) Ciardelli, F.; Pertici, P.; Vitulli, G.; Giaiacopi, S.; Ruggeri, G.; Pucci, A. *Macromol. Symp.* **2006**, *231*, 125−133. (b) Pehlivan, L.; Metay, E.; Laval, S.; Dayoub, W.; Demonchaux, P.; Mignani, G.; Lemaire, M. *Tetrahedron* **2011**, *67*, 1971−1976. (c) Takasaki, M.; Motoyama, Y.; Higashi, K.; Yoon, S.-H.; Mochida, I.; Nagashima, H. *Org. Lett.* **2008**, *10*, 1601−1604.

(25) Layek, K.; Kantam, M. L.; Shirai, M.; Hamane, D. N.; Sasaki, T.; Maheswaran, H. *Green Chem.* **2012**, *14*, 3164−3174.

(26) Vasilikogiannaki, E.; Gryparis, C.; Kotzabasaki, V.; Lykakis, I. N.; Stratakis, M. *Adv. Synth. Catal.* **2013**, *355*, 907−911.